Utilization of FEM model for steel microstructure determination

A Kešner[1], R Chotěborský[1], M Linda[2] and M Hromasová[2]

[1]Department of Material Science and Manufacturing Technology, Faculty of Engineering, Czech University of Life Sciences Prague
[2]Department of Electrical Engineering and Automation, Faculty of Engineering, Czech University of Life Sciences Prague
E-mail: kesner@tf.czu.cz

Abstract. Agricultural tools which are used in soil processing, they are worn by abrasive wear mechanism cases by hard minerals particles in the soil. The wear rate is influenced by mechanical characterization of tools material and wear rate is influenced also by soil mineral particle contents. Mechanical properties of steel can be affected by a technology of heat treatment that it leads to a different microstructures. Experimental work how to do it is very expensive and thanks to numerical methods like FEM we can assumed microstructure at low cost but each of numerical model is necessary to be verified. The aim of this work has shown a procedure of prediction microstructure of steel for agricultural tools. The material characterizations of 51CrV4 grade steel were used for numerical simulation like TTT diagram, heat capacity, heat conduction and other physical properties of material. A relationship between predicted microstructure by FEM and real microstructure after heat treatment shows a good correlation.

1. Introduction

Chisels, plows, tines, discs are agricultural tools that are used for soil cultivation around the world[1, 2].Agricultural tools are in direct contact with the soil. Contacting tools with soil will cause the abrasive wear mechanism. Abrasive wear causes undesirable material loss until the time when the tool is unable to perform a required function or if its destruction[3–5].The resulting microstructure is important for the abrasion resistance but also other mechanical properties such as hardness, toughness, strength[6–8].For these reasons, manufacturers of agricultural tools focus on optimizing the heat treatment process[9, 10].

Optimizing heat treatment means accurate design and adherence to temperatures and times. Compliance times and temperatures is provided by adjusting the production line[11, 12].It is important to focus on the exact design of the heat treatment. Agricultural tools are produced by austempering[13, 14].Experimental generation of austempering data is time-consuming and requires high costs.[15]. FEM models are used for the exact design of austempering. FEM models allow prediction of microstructure after heat treatment[16, 17].The construction of FEM models must include the effects of heat treatment such as heat transfer, nonlinear material properties, material shape, phase transformation[18]. The kinetics of austenite decomposition are important for describing the heat treatment process.Johnson-Mehl-Avrami-Kolgomorovequations are used to solve this problem for

diffusion transformations[19]. Koistinen-Marburgerequations are used to solve this problem for non-diffusion transformations[20].
The aim of this work is to design an algorithm that describes microstructure phases after heat treatment of 51CrV4 steel.The mathematical model is verified by experimental measurement.

2. Material and methods

Steel 51CrV4 (C=0.53, Mn=0.89, Si=0.26, Cr=1.02, Cu=0.13, V=0.12, P=0.012, S=0.025, Ni=0.08, Mo=0.02 (wt. %)) was used for modelling and experimental verification. The chemical composition was subtracted from the material sheet. Samples were prepared from steel Ø 30 mm rod. Sample sizes were adjusted to 25 mm x 10 mm x 45 mm. All samples were heated to 800 °C for 30 min. The cooling overview is shown in Table 1. After that samples were cut, grinded, polished and etched in Nital solution for metallography. Optical metallography and electron scanning metallography were used for a determination of phases into steel specimens.

Table 1. Overview of sample cooling

	cooling 1			cooling 2			cooling 3		
	temp. [°C]	**Medium [-]**	**Time [s]**	**temp. [°C]**	**Medium [-]**	**time [s]**	**temp. [°C]**	**Medium [-]**	**Time [s]**
V1	300	salt bath	40	300	air	1000	20	air	to 20°C
V2	300	salt bath	40	20	water	to 20°C	-	-	-
V3	400	salt bath	40	400	air	1200	20	air	to 20°C
V4	400	salt bath	40	20	water	to 20°C	-	-	-

The simulation algorithm was designed to predict the final microstructure after heat treatment – see Figure 1. The ElmerFem program was used for algorithm calculations. The Flowchart is shown in Figure 1 for the algorithm.

Dimensions 25 mm x 10 mm were selected for both experiment and model. The mesh was formed in the core of the object 12.5 mm and under the surface 22 mm x 5 mm. The boundary conditions are taken from the experimental part for heat treatment – see Table 1. Specific heat capacity, thermal conductivity was taken from the article Chotěborský and Linda [21].

Step Δt was chosen to solve the simulation. The **.vtu* file was created at each step Δt. The temperature change was stored in each part of the modeled sample at each stepΔt. "*M"*files present the number of simulation steps.

The transformation of austenite to martensite is a non-diffusional process. The non-diffusional process is calculated according toKoistinen–Marburger law – see equation 1 [22]. The changes from austenite to bainite, ferite and perliteare diffusional processes. Diffusional processes are calculated according to Johnson–Mehl–Avrami–Koglomorovequation – see equation 2 [20].

$$V_M = 1 - e^{-\alpha \times (M_S - T)} \tag{1}$$

$$V_{P,B,F} = 1 - e^{-K \times t^n} \tag{2}$$

where M_S– martensite start [s], T – temperature [K], t – time [s], K – overall rate constant [-], n – Avrami's exponent [-]

The calculations were made for the volume ratio of bainite*Vb*, martensite*Vm*, ferrite *Vf*, perlite *Vp* in each stepΔtaccording equations 3 to 6[21].

$$Vf = \sum_{i=1}^{n} -Kf \times Nf \times t^{Nf-1} \times e^{-Kf \times t^{Nf}} \times (1 - Vf_{max}) \tag{3}$$

$$Vp = \sum_{i=1}^{n} -Kp \times Np \times t^{Np-1} \times e^{-Kp \times t^{Np}} \times (1 - Vf) \quad (4)$$

$$Vb = \sum_{i=1}^{n} -Kb \times Nb \times t^{Nb-1} \times e^{-Kb \times t^{Nb}} \times (1 - Vf - Vp) \quad (5)$$

$$Vm = 1 - e^{-\beta \times (Tm_{start} - T)} \times (1 - Vf - Vp - Vb) \quad (6)$$

where *Kf, Kp, Kb* – overall rate constant of feritic, pearlitic and bainitic transformation that generally depends on temperature (-), *Nf, Np, Nb* – Avrami's exponent for feritic, pearlitic and bainitic transformation that depends on temperature (-)

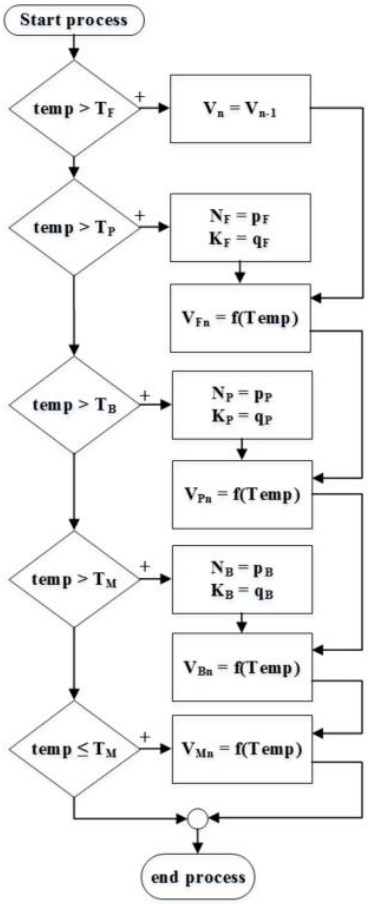

Figure 1. Flow chart for calculation of microstructure and hardness of steel after heat treatment

Conditions for formation of individual phases were taken from the TTT diagram for 51CrV4 steel. Parameters*Ni* and*Ki*are set forth in Kesneret al. [9]. The results were stored at a distance of 0.05 mm from the core to the edge of the sample.

3. Results and discussion

Bainite and martensite are only microstructures which have been identified in the results of experimental measurement and a mathematical model. The volume phases of perlite, ferrite, austenite were less representation than 0.01.For this reason, in this work only works with bainite and martensite in the next parts of this study.

Samples V1 and V3 wereaustempering in salt bath with a holding time in the air. Experimental measurements have shown bainitic structure with a very small amount of martensite for austempering– see Fig. 1.left. Sample V1 had a volume fraction 0.99 for bainite and 0.01 for martensite.Sample V3 had avolume fraction 0.98 for bainite and 0.02 for martensite.

Samples V2 and V4 were quenched in salt bath and then in water. The combination of bainite and martensite has been identified – see Fig. 1.right.A volume fraction of 0.67 martensite and 0.33 bainite was found for sample V2.A volume fraction of 0.76 martensite and 0.24 bainite was found for sample V4.The microstructure is shown in Figure 1 for the measured and calculated microstructure after heat treatment.

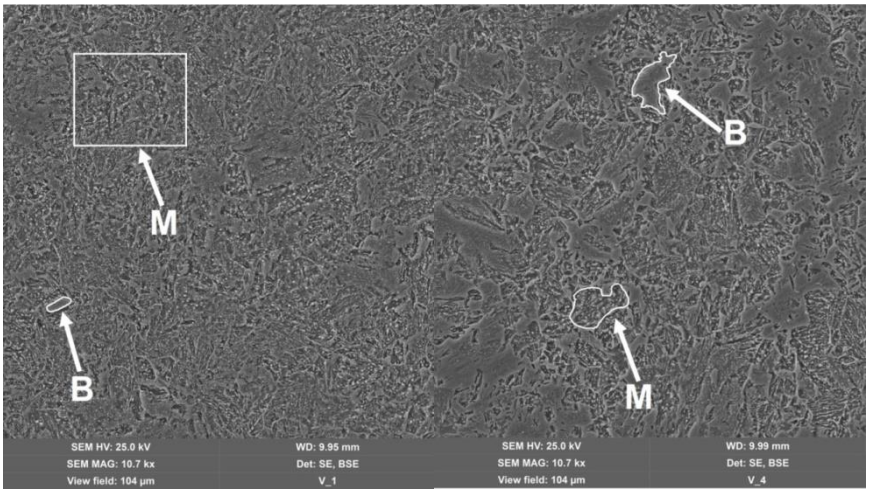

Figure 2. Microstructure with banite and martensite phases for steel51CrV4 –left for sample V1, rigth for sample V4

The comparison between the mathematical model and the experiment is shown in Fig. 3.for all samples. Samples V1 and V3 indicate good agreement between the mathematical model and experimental measurements. The results were displayed from the core to the edge of the sample at 0.2 mm for better clarity. The mathematical model indicates a volume fraction of 0.99 of bainite and 0.01 of martensite for samples V1 and V3. The difference between the mathematical model and the experimental measurement is the same for the sampleV1. The difference of 0.01 was found between the mathematical model and the experimental measurement.

Differences 0.26 for sample V2 and 0.16 for sample V4 were found between the mathematical model and the experimental measurement for the bainite and martensite phase. The cooling time was fast for these samples and this is one of the possible reasons for differences for the individual phases. Chemical composition can be another reason for high differences. The chemical composition has been taken from the material sheet into this work, and its batch may contain minor differences in some chemical elements. More heat treatment parameters could be used to refine the procedure in this work.

Difference was not found in the distribution of the individual phases from the core of the sample to its edge. Simsir and Gür[18]in their work dealt with the microstructure distribution. Their results show significant changes in the composition of the microstructure from the core of the sample to its edge during heat treatment in the salt baths and cooling in water. A larger sample size (ø60 mm) was used in their work. This may be one of the reasons why different microstructure across the sample is recorded in their work.

Chotěborský and Linda in their work were concerned with estimating the microstructure for the agricultural instrument. Differences are found between the mathematical model and the experimental measurement of phase representation in individual microstructures. Different values of specific heat capacity, heat flow, TTT diagram are given as possible causes. Different values may be due to different actual chemical composition of steel. This issue is the same for this work.

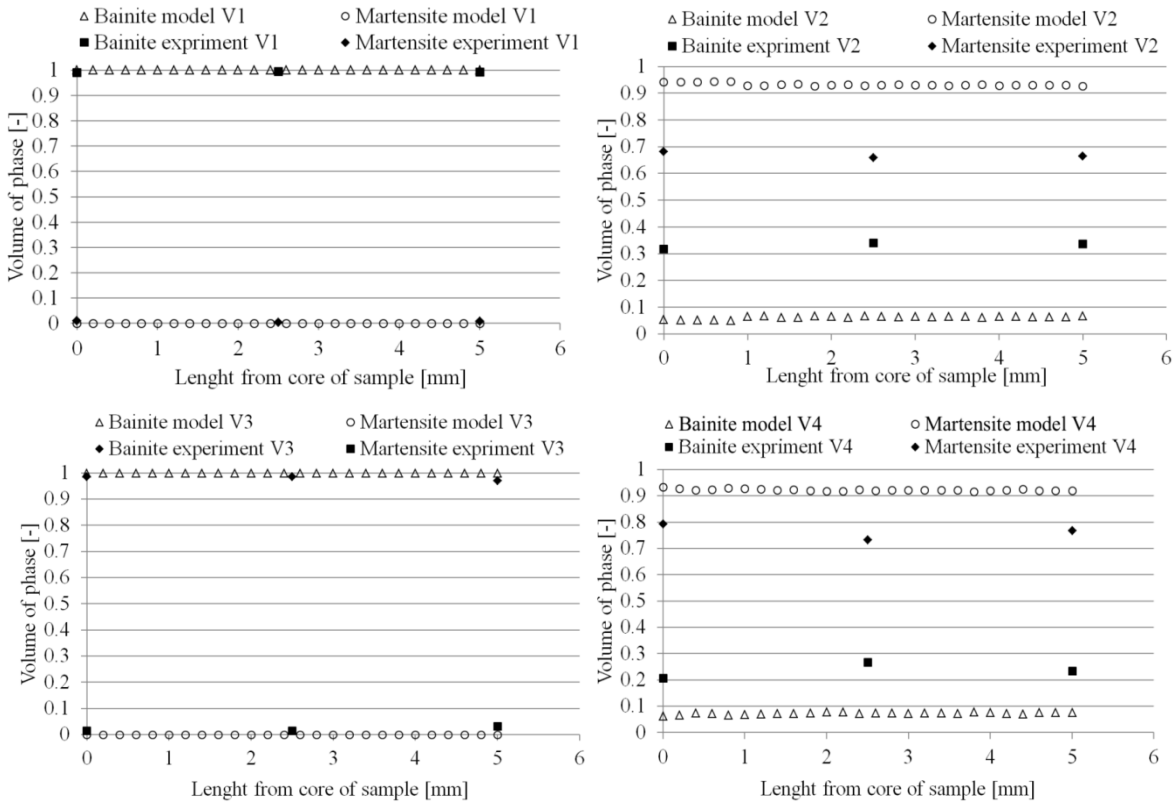

Figure 3. Dependency between volume of phase and length from core of sample

4. Conclusion

The mathematical model was assembled and experimentally verified for the detection of the microstructure of 51CrV4 steel. The results show a match for samples hardened in salt and then to the water. The resulting structure shows a bainitic structure with very small volume phase of martensite. The bainite structure is suitable for use in agricultural tools because it has good abrasion resistance. Samples hardened in a salt bath with a holding time in air showed 25% difference between the mathematical model and experimental measurements. These differences may be due to the different chemical composition of the steel. Chemical composition of steel affects boundary conditions such as heat capacity, heat flow and the values of the start and end of each phase during cooling. However, the above-mentioned procedure can be used to estimate the final microstructure composition after heat treatment.

References

[1] Votava J 2014 Usage of abrasion-resistant materials in agriculture*Journal of Central European Agriculture***15(**2), pp. 119–128.

[2] Rose D C, Sutherland W J, Parker C, Lobley M, Winter M, Morris C, Twining S, Ffoulkes CH, Amano T and Dicks L V 2016 Decision support tools for agriculture: Towards effective design and delivery*Agricultural Systems***149**, pp. 165–174.

[3] Bansal A, Zafar S and Sharma A K 2015 Microstructure and Abrasive Wear Performance of Ni-Wc Composite Microwave Clad. *Journal of Materials Engineering and Performance***24**(10), pp. 3708–3716.

[4] Elalem K and Li D Y 1999 Dynamical simulation of an abrasive wear process. *Journal of Computer-Aided Materials Design***6**(2), pp. 185–193.

[5] Chotěborský R, Hrabě P, Müller M, Savková J, Jirka M and Navrátilová M 2009 Effect of abrasive particle size on abrasive wear of hardfacing alloys. *Research in Agricultural*

*Engineering***55**(3).
[6] Wei M, Wang S, Wang L and Chen K 2011 Effect of Microstructures on Elevated-Temperature Wear Resistance of a Hot Working Die Steel. *Journal of Iron and Steel Research, International***18**(10), pp. 47–53.
[7] Weber S, Li J R and Theisen W 2010 Microstructure and wear properties of novel sintered cold work steel and related particle reinforced composite materials. *Materials Science and Technology***26**(12), pp. 1494–1502.
[8] Buchely M F, Gutierrez J C, León L M and Toro A 2005 The effect of microstructure on abrasive wear of hardfacing alloys. *Wear***259**(1–6), pp. 52–61.
[9] Kešner A, Chotěborský R and Linda M 2016 A numerical simulation of steel quenching. In : *Proceeding of 6th international conference on trends in agricultural engineering.*
[10] Votava J, Kumbár V and Polcar A 2016 Optimisation of Heat Treatment for Steel Stressed by Abrasive Erosive Degradation. *Acta Universitatis Agriculturae et Silviculturae Mendelianae Brunensis***64**(4), pp. 1267–1277.
[11] Müller M, Chotěborský R, Valášek P and Hloch S 2013 Unusual possibility of wear resistance increase research in the sphere of soil cultivation | Posebna mogućnost istraživanja povećanja otpornosti na trošenje u području obrade tla. *Tehnicki Vjesnik***20**(4).
[12] Archer D W and Reicosky D C 2009 Economic performance of alternative tillage systems in the northern corn belt. *Agronomy Journal***101**(2).
[13] Šolić S, Godec M, Schauperl Z and Donik Č 2016 Improvement in Abrasion Wear Resistance and Microstructural Changes with Deep Cryogenic Treatment of Austempered Ductile Cast Iron (ADI). *Metallurgical and Materials Transactions A***47**(10), pp. 5058–5070.
[14] Erdogan M, Kilicli V and Demir B 2007 Transformation characteristics of ductile iron austempered from intercritical austenitizing temperature ranges. *Journal of Materials Science***44**(5), pp. 1394–1403.
[15] Sinha V K, Prasad R S, Mandal A and Maity J 2007 A Mathematical Model to Predict Microstructure of Heat-Treated Steel. *Journal of Materials Engineering and Performance***16**(4), pp. 461–469.
[16] Deng D 2009 FEM prediction of welding residual stress and distortion in carbon steel considering phase transformation effects. *Materials & Design***30**(2), pp. 359–366.
[17] Kešner A, Chotěborský R and Linda M 2017 Determining the specific heat capacity and thermal conductivity for adjusting boundary conditions of FEM model. *Agronomy Research*. **15**, Special Is.
[18] Şimşir C and Gür C H 2008 A FEM based framework for simulation of thermal treatments: Application to steel quenching. *Computational Materials Science***44**(2), pp. 588–600.
[19] Martin D 2010 Application of Kolmogorov–Johnson–Mehl–Avrami equations to non-isothermal conditions. *Computational Materials Science***47**(3), pp. 796–800.
[20] Babu K and Prasanna Kumar T S 2014 Comparison of Austenite Decomposition Models During Finite Element Simulation of Water Quenching and Air Cooling of AISI 4140 Steel. *Metallurgical and Materials Transactions B***45**(4), pp. 1530–1544.
[21] Chotěborský R and Linda M 2015 FEM based numerical simulation for heat treatment of the agricultural tools. *Agronomy Research***13**(3),pp. 629–638.
[22] Pietrzyk M, Kusiak J, Kuziak R, Madej Ł, Szeliga D and Gołąb R. Conventional and Multiscale Modeling of Microstructure Evolution During Laminar Cooling of DP Steel Strips. *Metallurgical and Materials Transactions A***45**(13), pp. 5835–5851.

Acknowledgments
Supported by Internal grant 31140/1312/3114 agency of Faculty of Engineering, Czech University of Life Sciences in Prague.